

Article

Preparation of Robust Superhydrophobic Halloysite Clay Nanotubes via Mussel-Inspired Surface Modification

Yang Meng, Mingjie Wang, Mengfei Tang, Gonghua Hong, Jianmin Gao * and Yao Chen *

MOE Key Laboratory of Wooden Material Science and Application, College of Material Science and Technology, Beijing Forestry University, Beijing 100083, China; lxf_mengyang@bjfu.edu.cn (Y.M.); mannixwang@bjfu.edu.cn (M.W.); tmf9500@126.com (M.T.); honggonghua@bjfu.edu.cn (G.H.)

* Correspondence: jmgao@bjfu.edu.cn (J.G.); ychen@bjfu.edu.cn (Y.C.); Tel.: +86-010-6233-7960 (J.G.)

Received: 20 September 2017; Accepted: 25 October 2017; Published: 2 November 2017

Abstract: In this study, a novel and convenient bio-inspired modification strategy was used to create stable superhydrophobic structures on halloysite clay nanotubes (HNTs) surfaces. The polydopamine (PDA) nanoparticles can firmly adhere on HNTs surfaces in a mild environment of pH 8.5 via the oxidative self-polymerization of dopamine and synthesize a rough nano-layer assisted with vitamin M, which provides a catechol functional platform for the secondary reaction to graft hydrophobic long-chain alkylamine for preparation of hierarchical micro/nano structures with superhydrophobic properties. The micromorphology, crystal structure, and surface chemical composition of the resultant superhydrophobic HNTs were characterized by field emission scanning electron (FE-SEM), transmission electron microscopy (TEM), X-ray diffraction (XRD), Fourier transform infrared spectroscopy (FTIR), and X-ray photoelectron spectroscopy (XPS). The as-formed surfaces exhibited outstanding superhydrophobicity with a water contact angle (CA) of $156.3 \pm 2.3^\circ$, while having little effect on the crystal structures of HNTs. Meanwhile, the resultant HNTs also showed robust stability that can conquer various harsh conditions including strong acidic/alkaline solutions, organic solvents, water boiling, ultrasonic cleaning, and outdoor solar radiation. In addition, the novel HNTs exhibited excellent packaged capabilities of phase change materials (PCMs) for practical application in thermal energy storage, which improved the mass fractions by 22.94% for stearic acid and showed good recyclability. These HNTs also exhibited good oil/water separation ability. Consequently, due to the superior merits of high efficiency, easy operation, and non-toxicity, this bionic surface modification approach may make HNTs have great potentials for extensive applications.

Keywords: halloysite; nanotubes; mussel-inspiration; polydopamine; superhydrophobic surface modification

1. Introduction

In the past several years, superhydrophobic surfaces have attracted remarkable interest due to their unique wettability for potential applications in self-clean, anti-fog, anti-ice, anti-bacteria, oil-water separation, energy-storage, and drug-release [1–7]. To obtain these special wetting properties, surface modification has been developed to establish hierarchical micro/nano structures with hydrophobic chemical groups by learning from the exquisite tissues and organs in the biological world, such as lotus leaves and pond skater legs with super hydrophobicity [8]. Based on this bionic mechanism (i.e., the Wenzel and Cassie-Baxter models) [9], many superhydrophobic materials are fabricated from the traditional substrates such as wood, sponge, metal mesh, and fabric via appropriate physical and chemical approaches [10–13]. These functional materials have many advanced attractive merits and can be applied in both scientific and industrial fields. Most importantly, these raw materials are low cost and simple to acquire.

Halloysite clay nanotubes ($\text{Al}_2\text{Si}_2\text{O}_5(\text{OH})_4 \cdot n\text{H}_2\text{O}$, 1:1 layer aluminosilicates) (HNTs), as a kind of environmentally friendly and natural porous nanomaterial, are extensively used in many areas for numerous applications, such as polymer reinforcement, nano catalyst, and absorbing substrates for drug delivery, pollutants removal, and thermal energy storage [6,14–18]. However, natural HNTs are sensitive to moisture and it is easy to absorb water into the hollow cylinders because of the hydrophilic gibbsite octahedral sheet (Al–OH) groups existing on the internal surface [19]. This characteristic renders HNT difficult to disperse and a poor adsorptive capacity for hydrophobic organics, which limits its potential candidates as nanomaterials, especially for the preparation of polymeric nanocomposites and supporting porous materials. To combat this drawback, surface modification and functionalization has been used as a promising technique for artificial synthesizing hydrophobic HNTs, aiming to expand their application galleries [20].

Current research on superhydrophobic materials have focused on the utilization of various treatment process, mostly consisting of chemical vapor deposition (CVD), hot pulling, hydrothermal treatment, soft blasting, and sol-gel method for building lotus-leaf-like hierarchical structures [21–25]. However, as for HNTs, the superhydrophobic modifications are still at an embryonic stage mainly via combination of covalent bond with various alkylsilanes due to the similar siloxane groups (Si–O–Si) presenting on the external surface. For example, Liang et al. developed a novel superhydrophobic HNT with treatment of PDMS (polydimethylsiloxane) at 240 °C in a closed container, which had a high water contact angle (CA) of up to 157°, and it showed great potential to support phase change materials [6]. Wu et al. introduced ODTMS (octadecyltrimethoxysilane) into the surfaces of HNTs with reaction time of 90 h and a liquid marble agglomerated by modified HNTs was formed with a high CA above 160°, which could be applied in deliverable capsules and bioreactors [20]. Moreover, polyorganosilanes, octadecylsilane coordination with Ag nanoparticles, and polypropylene were also used as surface modifiers to acquire superhydrophobic HNTs [7,26,27]. Despite that these modified approaches were actually effective, in most cases, the fabrication routes suffered from a lot of limitations such as harsh processing conditions, tedious sophisticated synthesis environment, and specialized reaction apparatus, which exhibited the main hindrance holding back their extensive practical applications. Furthermore, the remaining waste liquor always comprised of acidic, alkali, and toxic organic solvents that may be harmful to environment. Therefore, the development of facile and “green” technologies that can change the polarity of HNTs, as well as enhance the durability is of great importance and urgently needed.

Fortunately, the strong adhesive mechanism of marine mussels was deciphered by Lee and his partners, finding that the catecholic amino acid, 3,4-dihydroxyphenyl-L-alanine (DOPA), was the primary functional molecular of mussel adhesive proteins (MAPs), which permitted this marine animal to firmly adhere to the surfaces of various substrates [28]. Inspired by MAPs, an easily accessible small molecule, α -(3,4-Dihydroxyphenyl)- β -aminoethane (dopamine), has been widely used to achieve multifunctional surfaces via oxidative self-polymerization in a mildly alkali solution (pH = 8.5) that is similar to the marine environment without adding extra toxic reagents [29]. This anchored polydopamine (PDA) layer that contains a large number of free catechol groups can serve as an “activated platform” for large-scale multiplicities of secondary reactions including reducing metal ions to form metallic nano-coatings and grafting with amino groups through Michael addition or Schiff base reactions [30]. In addition, the small dopamine molecule can easily enter into the inner space of HNTs, forming PDA functional layer both on the internal and external surfaces of HNTs [31]. Therefore, it is believable that this mussel-inspired method will definitely create the biomimetic micro/nano hierarchical structures on HNTs surfaces with robust superhydrophobic abilities.

In this study, we developed a convenient approach of transforming water-swallowable halloysite into superhydrophobicity with tremendous durability. Although some researchers have focused on the use of dopamine to create catechol functional coatings on the surfaces of HNTs [31–33], to the best of our knowledge, it has been no previous reports on using mussel-inspired catecholic layers to graft long chain alkylamines (octadecylamine) for the preparation of superhydrophobic HNTs

surfaces. In this process, dopamine can be immobilized to Al and Si atoms via non-covalent or covalent bonds, and be spontaneously physically polymerized into PDA, forming the “activated platform” to tightly adhere to the HNTs surfaces for forthcoming secondary reactions. Then, the anti-water octadecylamine (ODA) was linked to the PDA layer through Michael addition or Schiff base reactions, thus the hydrophobic surfaces were successfully established. Furthermore, Vitamin M (VM) was added into the reaction system acting as catalyst to require the ultimate superhydrophobic HNTs by hindering the formation of smooth PDA layers and improving the roughness of the PDA and ODA co-modified surfaces. The mussel-inspired surface modification method exhibits the following novelty merits and dramatic benefits. (1) The procedure of coating PDA onto HNTs were mild, simple, and highly efficient, which can be realized only through immersing HNTs in a weak alkaline dopamine solution at room temperature without intricate instruments; (2) The only solvents on this approach were water and ethanol, which was not toxic, sustainable, and friendly to environment; (3) Both the internal and external surfaces of HNTs were modified without damaging the original nanotube structures; and, (4) The resultant superhydrophobic HNTs surfaces exhibit a robust stability in diverse severe conditions, including boiling water, strong acid solution, organic solvent, high intensity sunlight, and ultrasonic cleaning, which made HNTs have outstanding potential as adsorption substrates for various applications such as thermal energy storage and wastewater treatment.

2. Materials and Methods

2.1. Materials

Natural halloysite clay nanotubes (HNTs) were obtained from Yanbo Mineral Processing Factory (Shijiazhuang, China). Dopamine hydrochloride (DA, assay $\geq 98.5\%$) and Vitamin M (VM, purity $\geq 97\%$) were supplied by Duly Biotech Co., Ltd. (Nanjing, China). Tris(hydroxymethyl) aminomethane (Tris, 99.9% purity) was purchased from Solarbio Science & Technology Co., Ltd. (Beijing, China). Octadecylamine (ODA, AR) and sodium hexametaphosphate (SHMP, AR) were obtained from Macklin Biochemical Co., Ltd. (Shanghai, China). Other reagents including deionized water, anhydrous ethanol, acetone, benzyl alcohol, hydrochloric acid, and stearic acid etc. were purchased from Beijing Chemical Reagent Factory (Beijing, China). All of the chemical reagents were used without further purification.

2.2. Superhydrophobic Surface Modification of the Halloysite Clay Nanotubes (HNTs) by Polydopamine (PDA) Coating and Octadecylamine (ODA) Grafting

The pristine HNTs were purified by dispersing into 2 mM hydrochloric acid solution (60 °C, 2 h) with energetic magnetic stirring to eradicate Fe impurities, followed by thoroughly washing, filtering, drying, and grinding, which was named as pure HNTs (P-HNTs). The catechol surface modified HNTs were obtained by submerging the white P-HNTs powders into dopamine aqueous solution (2.0 mg/mL) and then adding Tris buffer to alter pH to 8.5 with gently stirring for 12 h at room temperature (RT). After that, the black PDA decorating HNTs (PDA-HNTs) were obtained through centrifugation, completely rinsed with distilled water and vacuum dried at 60 °C. Next, the PDA-HNTs were immersed into ODA ethanol solution (10 mM) under mildly stirring at RT for 12 h, and then purified with anhydrous ethanol several times through centrifuge washing and vacuum dried at 60 °C. Finally, the hydrophobic ODA grafting HNTs (ODA-HNTs) were prepared. Furthermore, to increase the roughness of the PDA coatings, the dopamine aqueous solution was treated with VM (1 mg/mL) and was stirred for 12 h at 60 °C before use. After cooling to RT, the P-HNTs powders were soaked in this VM treatment dopamine solution, followed by the same modification process described above to obtain the VM assisted PDA surface modified HNTs and prepare the resultant superhydrophobic HNTs, which was labeled as VM/PDA-HNTs and VM/ODA-HNTs, respectively. The intermediate and final HNTs based on different preparation conditions were listed in Table 1.

Table 1. Surface modification of HNTs under different conditions ¹.

| No. | Labels | HNTs (g) | VM (mg/mL) | DA (mg/mL) | ODA (mmol/L) |
|-----|-------------|----------|------------|------------|--------------|
| 1 | P-HNTs | 5 | - | - | - |
| 2 | PDA-HNTs | 5 | - | 2 | - |
| 3 | VM/PDA-HNTs | 5 | 1 | 2 | - |
| 4 | ODA-HNTs | 5 | - | 2 | 10 |
| 5 | VM/ODA-HNTs | 5 | 1 | 2 | 10 |

¹ HNTs, halloysite clay nanotubes; VM, Vitamin M; DA, Dopamine; ODA, octadecylamine; P-HNTs, pristine HNTs; PDA-HNTs, PDA decorating HNTs.

2.3. Characterization of Surface Modified HNTs

The surface functional groups of the modified and unmodified HNTs samples were confirmed by Fourier transform infrared spectroscopy (FTIR, Vertex 70v (Bruker, Karlsruhe, Germany)). The sample waiting for test was pressed with potassium bromide (KBr) at a weight ratio of 1:100 forming a tablet. Then this tablet was analyzed in a mode of scanning range of 4000 to 500 cm^{-1} with 32 scans at 4 cm^{-1} resolution.

X-ray photoelectron spectroscopy (XPS, ESCALAB 250XI (Thermo Fisher Scientific Co., Ltd., Shanghai, China)) was operated using a monochromatic Al $K\alpha$ source (1486.7 eV) with power of 150 W. All spectra were obtained with a pass energy of 100 eV and the C 1s and N 1s regions were highlighted with high resolution scans.

X-ray diffraction (XRD, D8 Advanced (Bruker, Madison, WI, USA)) was carried out to analyze the HNTs structure and crystallite performances with a Cu $K\alpha$ radiation source of 1.5406 Å, and theta scans were collected ranging from 10° to 70° with a step size of 5°/min.

The morphologies of the HNTs samples was observed in field emission scanning electron microscopy (FE-SEM, FEI Quanta FEG 650 (Thermo Fisher Scientific Co., Ltd., Waltham, MA, USA)) at an accelerating voltage of 10 kV. Au layer was decorated on the samples surfaces before observation.

Transmission electron microscopy (TEM, JEM-2100F (JEOL Ltd., Tokyo, Japan)) was used to obtain the high resolution morphologies of single nanotubes at an acceleration of 80 kV. The samples were dispersed in ethanol followed by sonication. The diluted colloidal solution was dropped onto a copper grid and dried for imaging.

Water wettability were measured on a video-based contact angle meter (DSA100 (Kruss GmbH, Hamburg, Germany)) at 25 ± 1 °C and 50 ± 10 %RH. Contact angle (CA) test: a droplet of 3 μL deionized water was mildly put on the samples surfaces and recorded by a CCD camera at a rate of 24 frames s^{-1} . In addition, to verify the resultant superhydrophobic HNTs surfaces, the sliding angle (SA) was tested according to the method reported in the Reference [34]. A droplet of 10 μL deionized water was released on the samples surface, and then the platform was tilted gently until the droplet began to roll. The critical angle of the incline surface was recorded as sliding angle. Each sample was tested six different regions to eliminate any error.

2.4. Stability Test of the Superhydrophobic HNTs

Thermal and moist environment test: the superhydrophobic HNTs were added into a beaker of boiling water for 3 h, and then the sediments were filtrated and dried. Various solutions/solvents environment test: the resultant HNTs samples were placed into strong acidic/alkali solutions (HCl, pH = 3; NaOH, pH = 11), and diverse organic solvents for 24 h at room temperature, followed by rinsing, filtering, and drying. Outdoor solar radiation test: the samples placed on the roof platform and were exposed to sunlight for seven days. Ultrasonic cleaning test: the samples were immersed into a glass container of distilled water, followed by washing in an ultrasonic cleaner (KX-1860Q7, Kexi Instrument Equipment Co., Ltd., Beijing, China) for 1 h. All CAs of pre-test and post-test were measured to certify the environment stability.

2.5. The Application of Superhydrophobic HNTs for Solar Thermal Energy Storage

The pure HNTs (P-HNTs) and superhydrophobic HNTs (S-HNTs) were used as package substrates to prepare form-stable phase change composites for the application of solar thermal energy storage. Stearic acid (SA) was absorbed into the HNTs via vacuum impregnation, as established by previous researchers [6]. The thermal performances of the organic material and its composites including latent heats, and melting and solidification temperature were investigated by differential scanning calorimeter (DSC, DSC-204 (Netzsch Gerätebau GmbH, Wunsiedel, Germany)). The testing procedure was carried out by heating and cooling the samples from room temperature to 120 °C at a heating/cooling rate of 10 °C /min under a nitrogen stream rate of 40 mL/min. Moreover, the durability of the form-stable composites was observed through 300 continual melting-solidifying cycles.

2.6. The Application of Superhydrophobic HNTs for Oil/Water Separation

The self-designed facility apparatus was set up to separate water from trichloromethane (TCM)/water mixture (Figure S1). Before adding S-HNTs in the apparatus, a small piece of absorbent cotton was filled in the bottom of a funnel to block the absorbent powders. The system was operating through pouring the mixture into the funnel and then collecting the separated TCM in a conical flask. When there was no droplets dripping into the receiving conical flask, the purified water was poured back into the beaker, thus completing the oil/water separation.

3. Results and Discussion

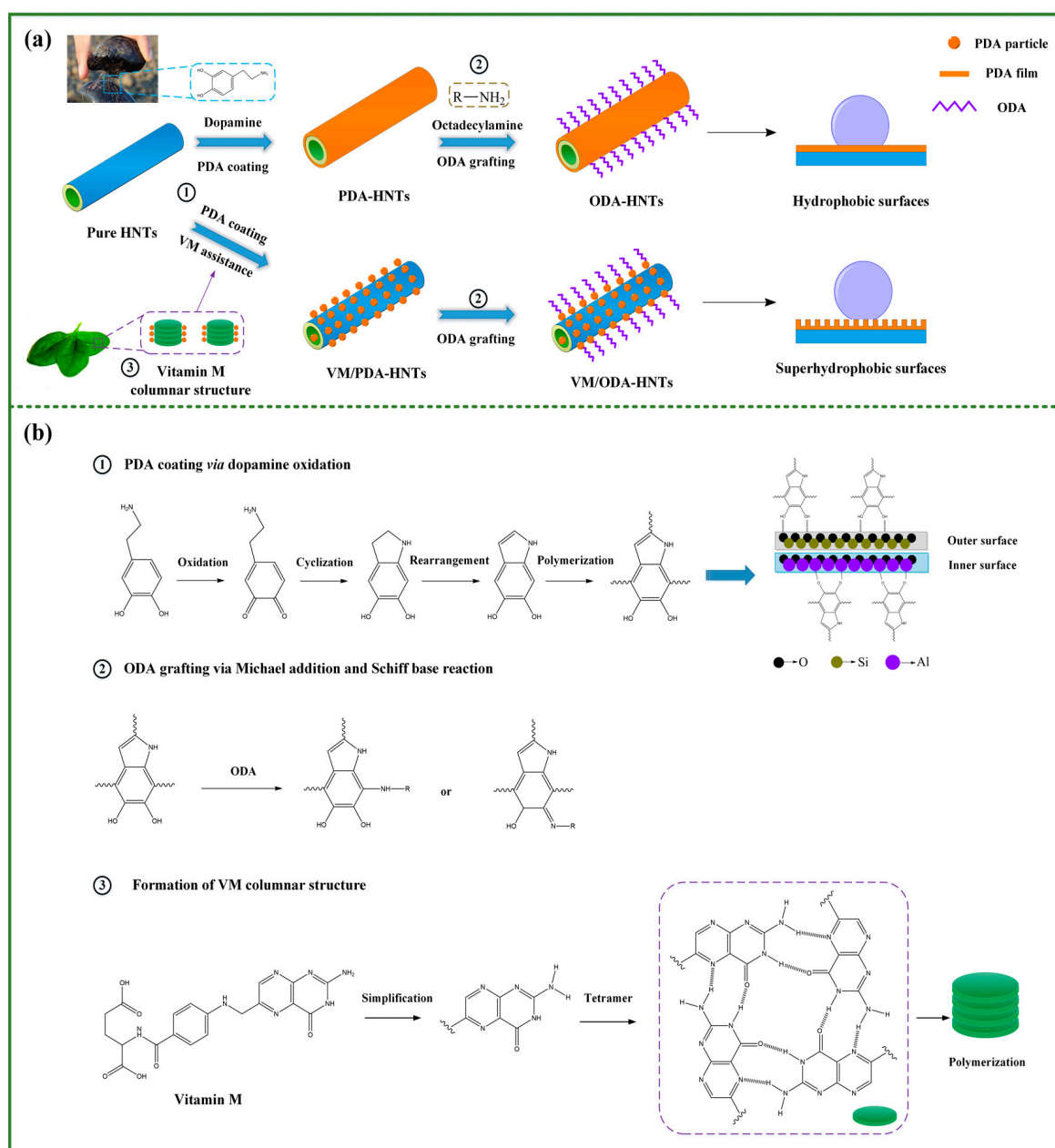
3.1. Preparation Process and Reaction Mechanism

The detailed mechanism of preparing the superhydrophobic HNTs via mussel inspired surface modification is shown in Scheme 1. HNTs can be easily decorated with catechol groups when immersed into an alkaline dopamine (DA) solution at room temperature. In this case, polydopamine (PDA) was synthesized via the oxidation and polymerization of DA, and firmly adhered on the HNTs surfaces, forming a robust, nanometer-thick, and smooth film, which was determined by Feng and his co-workers [31]. The secondary reaction to graft long-chain and anti-water alkylamine on PDA layers can introduce rough structure into HNTs substrates, which was the crucial factor for building superhydrophobic surfaces. However, the smooth PDA coatings obtained by typical method can hardly form primary obvious hierarchical structure, thus with the following secondary reaction, only hydrophobic surfaces would be achieved [35]. Various nanoparticles including noble metal (Ag) [36], metallic oxide (Fe_3O_4) [37], and silicon oxide [38] were incorporated through the catechol coordinate bonds and hydrogen bonds to create primary hierarchical structures on HNTs surfaces, however, this most-used approach suffered from a lot of disadvantages, such as high cost, time-consuming, and poor stability. Therefore, a direct way to control the roughness of PDA coatings without incorporation of nanoparticles was urgently needed.

Fortunately, it has been reported that bio-tetramers can serve as nano-templates for the preparation of nanomaterials [39]. In a basic environment, Vitamin M (VM) that was abundant in fresh vegetables can physically assemble into a tetramer through hydrogen bonds, and finally create columnar structures via π - π interactions [40]. As for the fabrication process of roughness PDA coatings, VM columnar structures disturbed the formation of continuous PDA film, while acted as structure-direction agents to help polymerize scattered PDA nanoparticles along the vertical direction [35]. According to this, we chose VM as an accelerator to control the procedure of PDA coating, which formed primary nano hierarchical structures followed by grafting ODA, and eventually transformed the surfaces properties of HNTs with robust superhydrophobicity.

To date, long chain alkylsilanes were frequently used to produce superhydrophobic surfaces. Nevertheless, this modified process only changed the external surface properties, and the hydrophilic internal surfaces still remained because of the incompatibilities between the gibbsite octahedral sheet groups and alkylsilanes [20]. In addition, the natural nanostructure may suffer the risk of being

damaged due to the harsh reaction conditions. Herein, the mussel inspired surface modification was carried out under mild environment, which changed the hydrophilic properties both on the internal and external surfaces without damaging the original nanotube structures. The hydrophobic external surfaces improve the dispersion of HNTs, meanwhile the hydrophobic internal surfaces enhanced the absorption ability for oil and anti-water compounds. The resultant superhydrophobic surfaces exhibited prominent stability in numerous harsh environments owing to the superior adhesion of catechol groups.



Scheme 1. The production process and reaction mechanism of superhydrophobic halloysite nanotube (HNTs). (a) Surface modification procedure of HNTs; (b) Chemical reaction mechanism: ① Illustration of oxidation polymerization and probable connection mode of dopamine on HNTs [33]; ② The mechanism of grafting octadecylamine (ODA) to obtain roughness surface via Michael addition and Schiff based reactions; ③ The formation of Vitamin M (VM) tetramer and the resultant columnar structure.

3.2. Micromorphology and Surface Chemical Composition Analysis

The dispersed state and micromorphology of HNTs before and after surface modification were observed by FE-SEM, as presented in Figure 1. Natural HNTs shows nanotube structures with massive block impurities stacked together (Figure 1a), and these unique nanotube structures are completely preserved and easily recognized after the purification of acid-heat pretreatment (Figure 1b), which is the same as the study to treat HNTs with sulfuric acid [41]. Figure 1c,d exhibit the morphological changes of PDA decorated HNTs, and it is observed that the tubular structure of the PDA-HNTs and VM/PDA-HNTs become thicker than that of the P-HNTs, while the dispersibility is improved, indicating that PDA is well anchored on the HNTs surfaces [42,43]. After grafting with ODA, the hydrophilic surface properties of P-HNTs were transformed by the hydrophobic long-chain alkyl groups in ODA molecules, and excitingly, a large number of single continuous or intact HNTs fibers distinctly appeared in Figure 1e,f. The agglomeration of HNTs fibers was notably decreased.

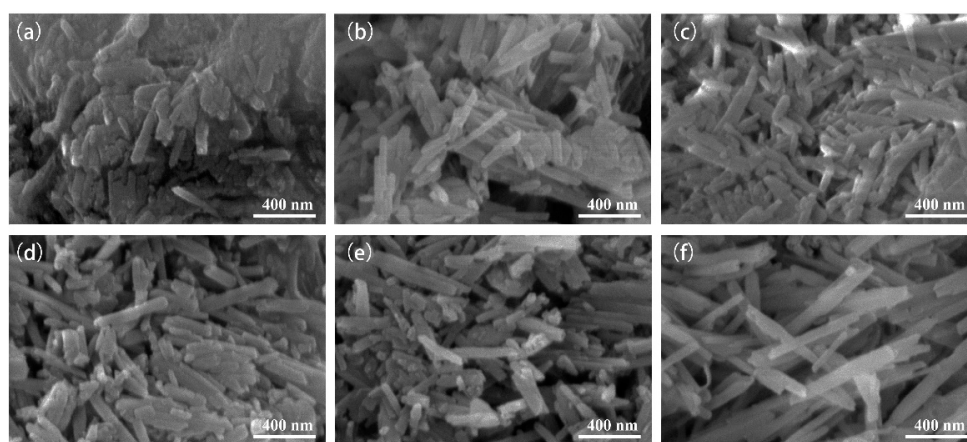


Figure 1. Field emission scanning electron microscopy (FE-SEM) images of the (a) pristine halloysite clay nanotubes (HNTs); (b) pure HNTs (P-HNTs); (c) polydopamine (PDA) decorating HNTs (PDA-HNTs); (d) PDA-HNTs assisted with Vitamin M (VM/PDA-HNTs); (e) octadecylamine (ODA) grafting HNTs (ODA-HNTs); and (f) ODA-HNTs assisted with Vitamin M (VM/ODA-HNTs).

The micromorphology images of single halloysite clay nanotube (HNT) samples are presented in Figure 2. As shown in Figure 2a, it could be clearly observed that pure HNTs were tubular in shape with a smooth surface and comprised a distinct hollow space running longitudinally along the tube, revealing the double-layered and open-ended characteristics [44]. The external diameters and lengths of P-HNTs were about 30–60 nm and 0.15–1.0 μm , respectively. After surface modified with PDA, the hollow space was difficult to be distinguished and the cylinder wall of the PDA coated HNT was significantly thicker than that of pure HNT (Figure 2b). This may be due to the self-polymerized PDA layers in both internal and external surfaces [32]. When compared to the PDA-HNTs, the edges and surfaces of ODA-HNTs became irregularity, which was ascribed to the long-chain alkylamine grafting onto the PDA-HNTs surfaces (Figure 2c).

The XRD patterns of pure HNTs and surface modified HNTs were observed, as shown in Figure 3. The typical characteristic diffraction peaks of HNTs located at the 2θ angles of 12.2° , 18.0° , 19.8° , 24.8° , 26.6° , 30.0° , 34.8° , 38.3° , 52.5° , 55.4° and 62.3° were all found in P-HNTs, which demonstrated that the crystalline structure of HNTs can hardly be damaged after acid purification [31,45]. Apparently, the following process of PDA and ODA surface modification had no obvious effects on these typical crystal diffraction peaks of P-HNTs with respect to both the shapes and 2θ angles, implying that the original crystal structure of HNTs was not altered.

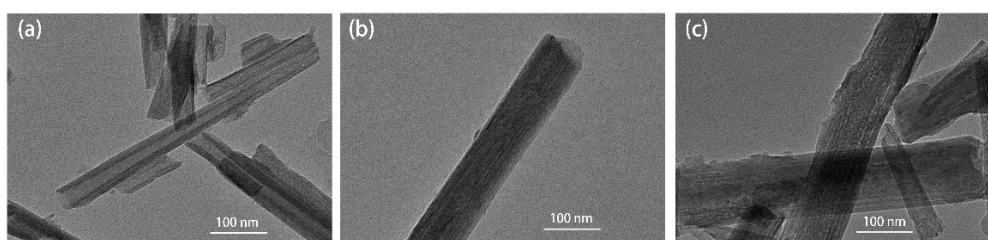


Figure 2. Transmission electron microscopy (TEM) images of the (a) P-HNTs; (b) PDA-HNTs; and (c) ODA-HNTs.

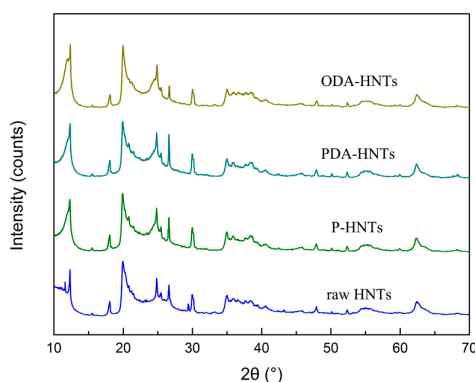


Figure 3. X-ray diffraction (XRD) patterns of P-HNTs, PDA-HNTs, ODA-HNTs, and VM/ODA-HNTs.

The FTIR spectra of the P-HNTs, PDA-HNTs, ODA-HNTs, and VM/ODA-HNTs were investigated to confirm the structures and chemical groups of pure and surface modified HNTs as shown in Figure 4. In the spectra of P-HNTs, two strong absorption peaks appeared at 3698 cm^{-1} and 3625 cm^{-1} , which were ascribed to the stretching vibration of AlO–H bonds. As for the HNTs spectra in fingerprint region ranging from 2000 cm^{-1} to 500 cm^{-1} , the peaks at 1091 cm^{-1} and 1031 cm^{-1} represented the in-plane stretching vibration of Si–O bonds and symmetric stretching of Si–O–Si was observed at 793 cm^{-1} . The spectral bands at 910 cm^{-1} and 690 cm^{-1} correspond to the stretching vibration of Al–OH bonds. Besides, the perpendicular stretching and deformation banding vibration of Si–O–Al were obviously found at 757 cm^{-1} and 537 cm^{-1} , respectively. These peaks were in common with the FTIR spectra of HNTs investigated by Yuan et al. [46], indicating that the typical structures and chemical groups of HNTs were retained after the purification of acid treatment. After being treated by PDA, there remained little changed in the characteristic peaks of pure HNTs. The new peaks at 3422 cm^{-1} , $2940\text{ cm}^{-1}/2875\text{ cm}^{-1}$, and 1650 cm^{-1} that were found in PDA-HNTs were attributed to the stretching vibrations of –OH groups, non-symmetric/symmetric stretching vibrations of –CH₂ groups, and the stretching vibrations of aromatic C=C groups, respectively, which proved that PDA had been successfully decorated on the HNTs surfaces [32,47]. In comparison to the spectra of PDA-HNTs, the absorption peaks at 2940 cm^{-1} and 2875 cm^{-1} in ODA-HNTs were enhanced, which was ascribed to the secondary reaction of grafting long chain alkyl amine in PDA platforms. Excitingly, although VM was added to the reaction system, the location and intensity of characteristic peaks in VM/ODA-HNTs were almost identical to those in ODA-HNTs, indicating that VM simply acted as a promoter instead of reacting with PDA and HNTs.

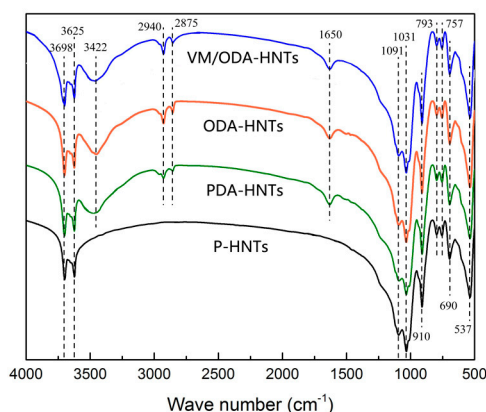


Figure 4. The Fourier transform infrared spectroscopy (FTIR) spectra of the P-HNTs, PDA-HNTs, ODA-HNTs and VM/ODA-HNTs.

The surface chemical changes of HNTs after mussel inspired modification were determined by investigating the XPS spectra of nanotube surfaces. Figure 5a presents the low resolution XPS wide scan spectra of PDA-HNTs and ODA-HNTs. As shown in Figure 5a, the characteristic peaks of O 1s, Si 2p/2s, and Al 2p/2s were all observed in these two samples, which were attributed to the elements O, Si, and Al in HNTs. In the case of unmodified P-HNTs, carbon impurity (C 1s peak) was detected on the nanoclay surfaces as shown in Figure S1, which could be assigned to the contamination of the oxide surface deriving from the atmosphere or in the wet process [48]. Excitingly, the signals of N appeared in the curve of PDA-HNTs, indicating that the PDA layer was successfully decorated on the HNTs surfaces. When compared with PDA-HNTs, the higher at. % of elements C (26.45%) and N (1.57%) were found in ODA-HNTs (Table S1), which was ascribed to the long-chain alkylamine grafting onto the PDA-coated HNTs. Figure 5b shows the high resolution XPS spectra of C 1s core-level spectra of PDA-HNTs. This C1 core-level spectra can be curved-fitted to three peak components corresponding to binding energy (BE) at 284.4 eV for C–C, C=C, and C–NH₂ species, at 285.7 eV for C–O and C–N species, and at 287.7 eV for C=O species, respectively, which were in well accordance with reported functional groups species of polydopamine [47]. Interestingly, the contents of C=O species were much lower than that of polydopamine coating on other substrates (>10%) [49], only 1.83% in PDA-HNTs (Table S2). This may be due to the high surface area of HNTs that can inhibit the change of dopamine from phenol to quinone [31]. Figure 5c,d exhibit the N 1s core-level spectra of the PDA-HNTs and ODA-HNTs. The N 1s core-level of PDA-HNTs was peak-fitted into three components, including primary amine species (R–NH₂, 401.8 eV), secondary amine species (R₁–NH–R₂, 399.9 eV), and tertiary or aromatic amine species (C=NR, 398.6 eV), respectively [32,50]. As for ODA-HNTs, the contents of secondary (36.31%) and tertiary/aromatic amine (22.20%) species spectrum were enhanced (Table S3) due to octadecylamine grafting onto PDA-HNTs surface via Michael addition or Schiff base reactions, resulting in two different kinds of resultant products, as illustrated in Scheme 1. Combining with the FT-IR analysis, these results suggested that the HNTs surface were successfully modified through introducing PDA layers as a platform for grafting long-chain alkyl groups to acquire hydrophobic performance.

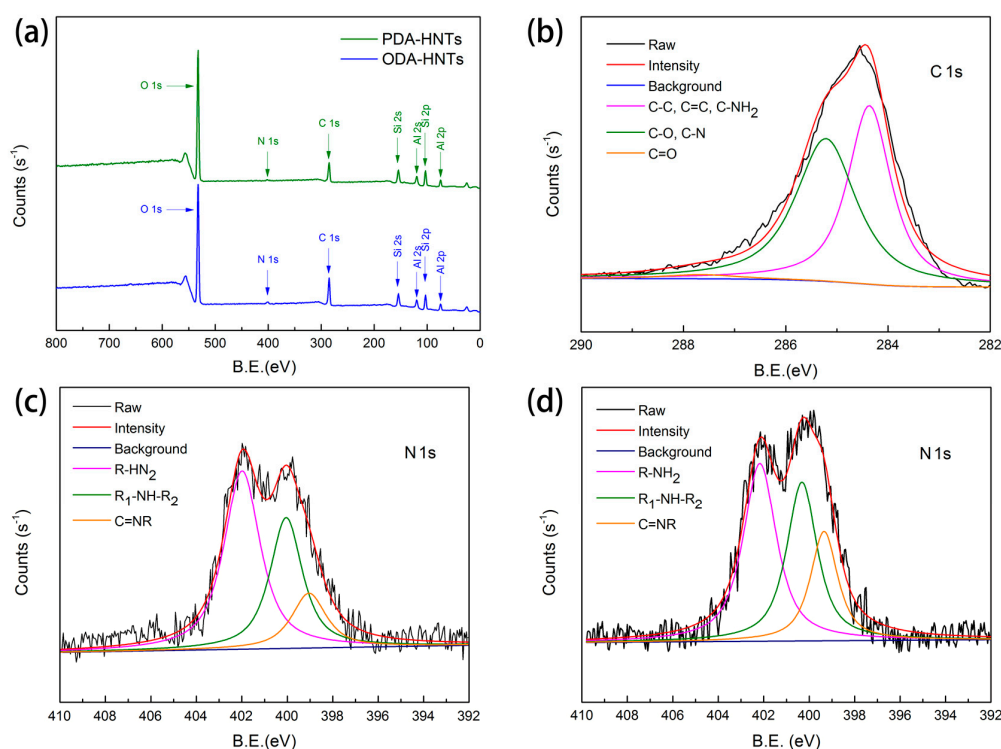


Figure 5. X-ray photoelectron spectroscopy (XPS) wide-scan and high resolution spectra of HNTs samples. (a) wide-scan XPS spectra of PDA-HNTs and ODA-HNTs; (b) C 1s core-level of PDA-HNTs; (c) N 1s core-level of PDA-HNTs; (d) N 1s core-level of ODA-HNTs.

3.3. Superhydrophobic Property and Environmental Durability

To evaluate the wettability properties of HNTs samples, the contact angle (CA) and sliding angle (SA) were tested by releasing water droplets of defined volume on the surface of flattened HNTs powders, and micrographs were recorded by CCD camera, as shown in Figure 6. The CA values of P-HNTs were less than 10° (Figure 6a), indicating that the pure halloysite was hydrophilic. When coating PDA on HNT surface, the CA increased to $46.7 \pm 3.1^\circ$ (Figure 6b), which was similar to the reported CA values of 46.9° [31]. After the following reaction for grafting long-chain alkylamine, the surface property of HNT was changed from hydrophilic to hydrophobic, with CA values of $112.3 \pm 3.3^\circ$ (Figure 6d). Interestingly, with the help of VM, the mean CA values of VM/PDA-HNTs ($57.2 \pm 4.3^\circ$, Figure 6c) were marginally higher than these of PDA-HNTs. Correspondingly, the highest CA values of $156.3 \pm 2.3^\circ$ (Figure 6e) were observed in VM/ODA-HNTs with SA values of $4.5 \pm 0.4^\circ$ (Figure 6f), demonstrating that the resultant superhydrophobic surface was finally achieved. It may be ascribed to the self-assembly of VM, forming a columnar structure that can act as a template to induce PDA nodules in the vertical direction, thus creating rough PDA coatings on the surface of HNTs [39,40]. In addition, the anti-water long-chain alkyl groups were grafted onto this rough surface. Consequently, the resultant superhydrophobic structures were successfully built on the HNTs, as illustrated in Scheme 1.

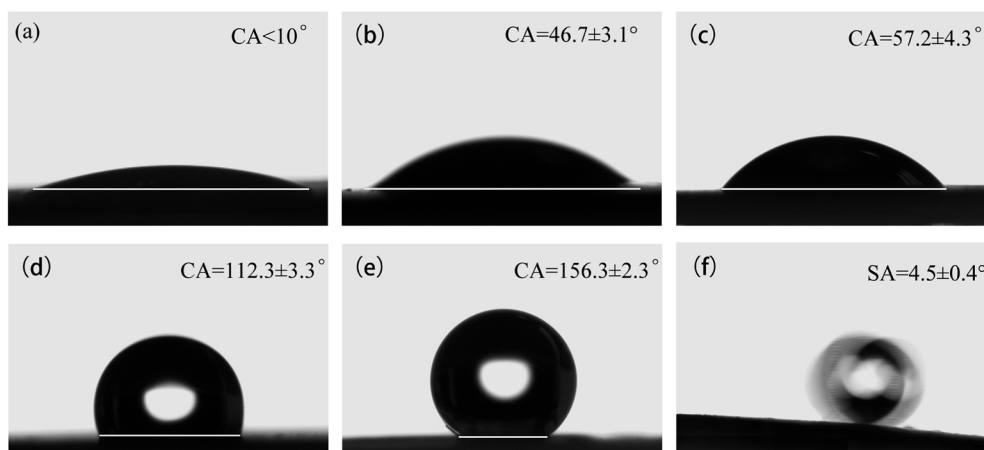


Figure 6. Micrographs of 3 μL deionized water droplets on the plane surfaces of (a) P-HNTs; (b) PDA-HNTs; (c) VM/PDA-HNTs; (d) ODA-HNTs; and (e) VM/ODA-HNTs; 10 μL deionized water droplets on the incline surfaces of (f) VM/ODA-HNTs.

Figure 7a exhibits the changes of CAs on the surface of flattened HNTs powder samples over time. The CAs on P-HNTs decreased quickly in 15 s, and slowly reached the equilibrium in the next 60 s. After coating PDA on HNT surface, the water resistance performance of PDA-HNTs became better at the beginning of the contact in comparison with the pure one. However, with time going on, the CAs continued to decline in 150 s, and finally got to the minimum value below 10° . These results suggested that simple dopamine as a modifier can hardly generate the hydrophobic layers on HNT surface, which was ascribed to the hydrophilic groups (e.g., amino, hydroxyl) existing on the PDA molecule [30]. The CAs of ODA-HNTs decreased from about 120° to 110° in 150 s, which presented hydrophobic performance. In the case of VM, the CAs on VM/ODA-HNTs surfaces exhibited no apparent change for this period of time, and all were maintained over 150° after 150 s. These phenomena can be easily observed in the optical photographs. When dropped on the hydrophilic HNTs surface (separate samples of P-HNTs, PDA-HNTs, and VM/PDA-HNTs), the water droplets immersed into the powders, leaving an agglomerated and wet surface (Figure 7b–d). In contrast, the water droplets remained their round shape on the hydrophobic HNTs surface (Figure 7e,f). Especially, the spherical water spot similar to that on lotus leaf was founded on the VM/ODA-HNTs surfaces.

To evaluate the environment durability performance of superhydrophobic HNTs, various tests were conducted corresponding to different harsh conditions. As shown in Figure 8a, the CAs of VM/ODA-HNTs were all maintained above 150° after immersing these superhydrophobic samples into diverse chemical conditions including solutions of HCl (pH = 3) and NaOH (pH = 11), acetone, ethanol, dioxane, and trichloromethane (TCM) for 24 h at room temperature, and boiling water for 3 h, which demonstrated the resultant superhydrophobic HNTs had great chemical resistances. Figure 8b shows the variation of CAs after ultrasonic washing the superhydrophobic HNTs samples with 60 min. These values were all above 150° at different ultrasonic times, indicating that the loaded PDA layers had strong adhesive properties, just like the mussel byssuses. The outdoor durability tests were carried out by exposing the superhydrophobic HNTs samples to sunlight, and the CAs results were recorded at 24 h interval as presented in Figure 8c. Apparently, all of the values remained at about 150° after solar radiation, suggesting that the samples had excellent stability to endure the harsh outdoor environment.

To sum up, diverse superhydrophobic surfaces have been successfully constructed on various substrates. However, many of them had poor environment durability, especially in ultrasonic washing, organic solvents, and strong acidic/alkaline solutions, which limited their practical applications [51,52]. In this study, this bio-inspired modification method can create a stable and robust superhydrophobic structure on HNTs surfaces, which can conquer various harsh conditions.

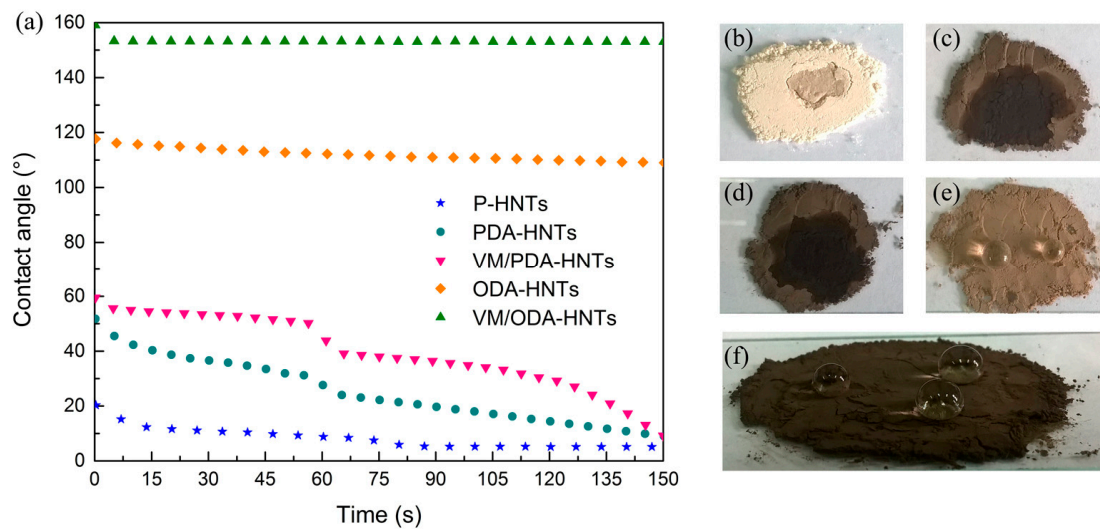


Figure 7. Water wettability properties characterization. (a) Contact angle testing results as a function of time for HNTs samples; and optical photographs of deionized water droplets on (b) P-HNTs; (c) PDA-HNTs; (d) VM/PDA-HNTs; (e) ODA-HNTs; and (f) VM/ODA-HNTs.

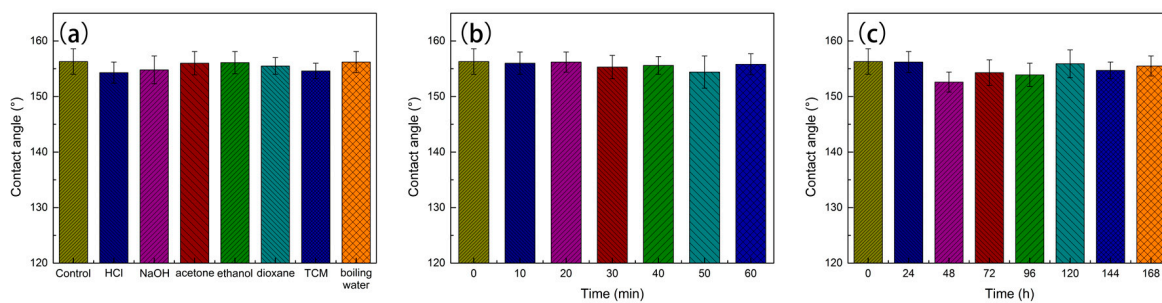


Figure 8. Environment durability performance of superhydrophobic HNTs. (a) contact angles (CAs) for HNTs samples immersed into different chemical solutions for 24 h; (b) CAs as a function of time of ultrasonic washing in water; (c) CAs as a function of outdoor solar radiation exposure time.

3.4. Application Analysis of Superhydrophobic HNTs

Phase change thermal storage technology, using phase change material (PCM) to store and release the intermittent or surplus heat, is one of the most efficient methods for solar thermal storage [53]. Many Organic materials, such as paraffin, PEG, and stearic acid (SA), dominate the PCMs utilization due to their superior merits of high capacity and good chemical stability [54]. However, the leakage occurring in solid-liquid phase change transition limits their practical applications. To combat this drawback, various porous materials have been exploited as package substrates for preparing form-stable PCM composites [55]. Halloysite as a kind of natural nanomaterial has the advantages of low cost, easy accessibility, and high porosity, which can be used as a packaging material to absorb PCMs [56]. However, its original hydrophilic property makes it incompatible with the hydrophobic organic compounds. As shown in Figure 9 and Table 2, pure HNTs (P-HNTs) can only absorb stearic acid with the maximum mass fraction of 46.2%. In this case, the latent heats of melting and cooling of SA/P-HNTs were 68.12 J/g and 60.75 J/g, respectively. After bio-inspired superhydrophobic surface modification, superhydrophobic HNTs (S-HNTs) based SA composites (SA/S-HNTs) presented the higher maximum package mass fraction (58.6%) than SA/P-HNTs, as well as the melting (88.42 J/g) and the cooling (79.37 J/g) latent heats, which were improved by 22.94%, 29.80%, and 30.65%, respectively. This may be attributable to the good interface affinity between SA and S-HNTs. Besides, the resultant form-stable PCM composite also showed an excellent thermal stability. The latent heats of SA/HNTs

were 85.23 J/g for melting and 75.61 J/g for cooling, presenting a decrease of only 3.19 J/g and 3.76 J/g, respectively, which showed a good potential application in thermal energy storage. These results were close to the research about superhydrophobic HNTs based phase change material composites via the surface modification of polydimethylsiloxane [6].

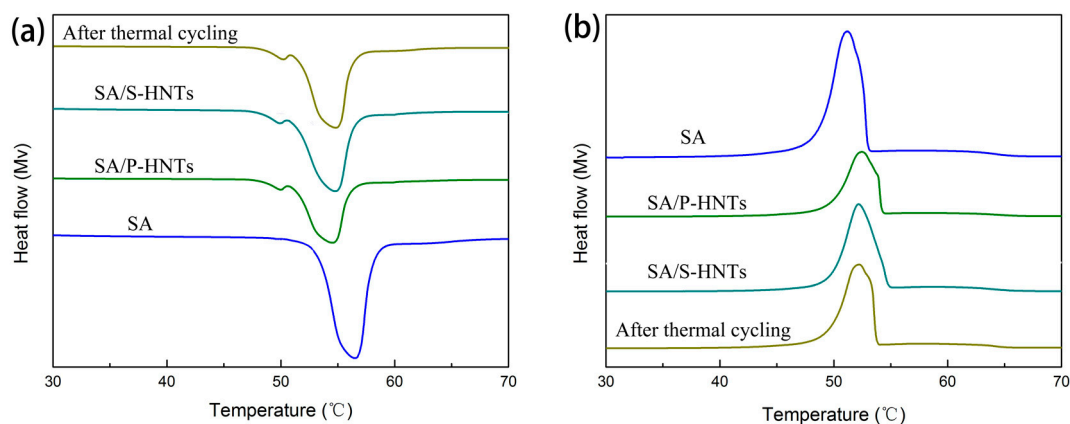


Figure 9. Differential scanning calorimeter (DSC) curves for heating (a) and cooling; (b) of stearic acid (SA) and form-stable composite phase change materials (PCM).

Table 2. Thermal properties of stearic acid (SA) and the related form-stable composite phase change materials (PCM) composites ¹.

| Samples | W/% | Heating | | | Cooling | | |
|----------------------|------|------------|-----------|-------------------------------|------------|-----------|-------------------------------|
| | | Onset T/°C | Peak T/°C | Latent Heat/J g ⁻¹ | Onset T/°C | Peak T/°C | Latent Heat/J g ⁻¹ |
| SA | 100 | 52.81 | 56.62 | 184.30 | 52.96 | 51.15 | 177.90 |
| SA/P-HNTs | 46.2 | 51.03 | 54.52 | 68.12 | 54.12 | 52.45 | 60.75 |
| SA/S-HNTs | 58.6 | 51.52 | 54.82 | 88.42 | 54.43 | 52.15 | 79.37 |
| SA/S-HNTs 300 cycles | 58.0 | 51.31 | 54.74 | 85.23 | 54.02 | 52.20 | 75.61 |

¹ W represents the mass fraction of SA in the as-prepared form-stable composites. S-HNTs, superhydrophobic HNTs.

Oil/water separation technique is one of the most favorable methods of wastewater treatment [35,37]. Due to the abundant pore structures and high surface area, HNTs may be used as an absorbent substrate to separate water from the oil/water mixture. However, the natural HNT has no selective absorption for oil and water. Hence, it can only be used to remove water-soluble cationic and anionic contaminants from wastewater [57]. Excitingly, the resultant superhydrophobic HNTs (S-HNTs) that have unique water resistance property and strong oil-absorbing capacity are promisingly suitable as a filter for oil/water separation. As shown in Figure 10, trichloromethane (TCM, dyed with Oil Red O)/water mixture was poured onto the facility apparatus, then TCM penetrated through the S-HNTs layer spontaneously, and was finally dripped into the collecting conical flask. The separated water was blocked by the S-HNTs, remained inside the funnel, and then poured back into the beaker. The complete oil/water separation process can be achieved with a simple way and without demand of extra force, which showed that S-HNTs have great potential for use in oil/water separation.

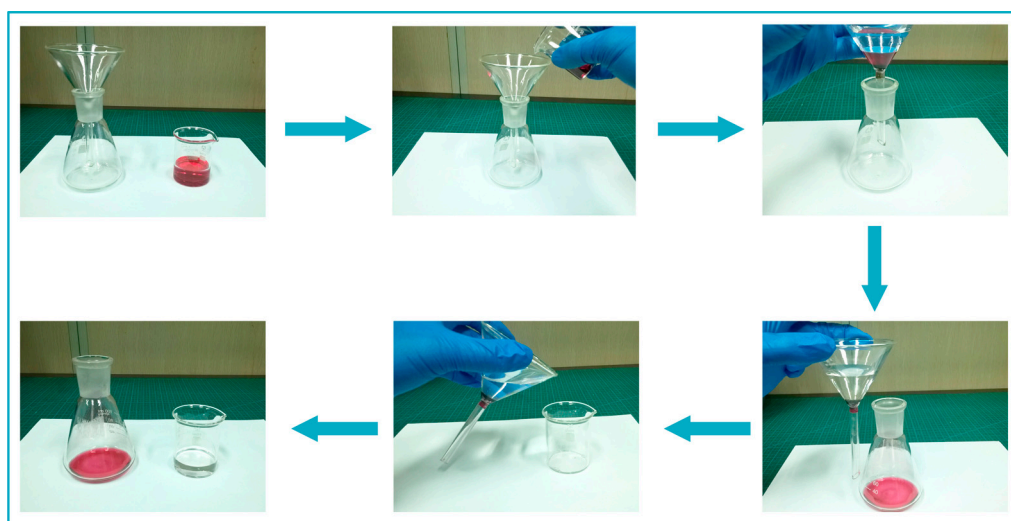


Figure 10. Optical photographs of the oil/water separation process by the superhydrophobic HNTs.

4. Conclusions

A novel and facile method to construct a superhydrophobic surface on HNTs was developed, inspired by strong adhesion proteins in mussel byssus. The synthesized PDA layers assisted with VM in the first step serviced as a platform for secondary reaction to graft long-chain alkylamine, forming biomimetic hierarchical micro/nano structures on HNTs surfaces with superhydrophobic abilities. The successful surface modification of HNTs with dopamine and octadecylamine was verified by TEM, FTIR, and XPS. With the process of superhydrophobic surface modification, the as-prepared HNTs presented good dispersibility, which was determined by SEM images. XRD results showed that this bio-inspired modification method had little effect on the crystal structures of HNTs. In addition, the resultant superhydrophobic HNTs possessed robust stability under harsh conditions, including strong acidic/alkaline solutions, organic solvents, water boiling, ultrasonic cleaning, and outdoor solar radiation. As for practical applications in thermal energy storage, the novel HNTs had excellent packaged capabilities of phase change materials, which improved the mass fractions by 22.94% for stearic acid in comparison of pure HNTs and also demonstrated good recyclability. The superhydrophobic HNTs also presented a special ability of oil-water separation. In brief, this bionic surface modification approach with advantages of high efficiency, easy operation, and non-toxicity changed the hydrophilicity of HNT surface, making it have great potentials for extensive applications.

Supplementary Materials: The following are available online at <http://www.mdpi.com/2076-3417/7/11/1129/s1>, Figure S1: Diagram of oil/water separation system, Figure S2: XPS wide-scan spectra of P-HNTs, Table S1: XPS total elements survey of HNTs samples, Table S2: Functional group percentages of C 1s in PDA-HNTs high resolution XPS spectra, Table S3: Functional group percentages of N 1s in high resolution XPS spectra.

Acknowledgments: The study was supported by the “Fundamental Research Funds for the Central Universities (No. 2017ZY42)”, “National Natural Science Foundation of China (No. 31400498)”, and “National Natural Science Foundation of China (No. 51572028)”.

Author Contributions: Yang Meng, Jianmin Gao, and Yao Chen conceived the project and designed the experiments; Yang Meng wrote the main manuscript text; Yang Meng, Mingjie Wang, Mengfei Tang, and Gonghua Hong performed the experiments and analyzed the data; Jianmin Gao and Yao Chen supervised and directed the project; all authors reviewed the manuscript.

Conflicts of Interest: The authors declare no conflict of interest.

References

1. Xu, Q.; Zhang, W.W.; Dong, C.B.; Sreepasad, T.S.; Xia, Z.H. Biomimetic self-cleaning surfaces: Synthesis, mechanism and applications. *J. R. Soc. Interface* **2016**, *13*. [[CrossRef](#)] [[PubMed](#)]

2. Shang, Q.Q.; Zhou, Y.H. Fabrication of transparent superhydrophobic porous silica coating for self-cleaning and anti-fogging. *Ceram. Int.* **2016**, *42*, 8706–8712. [[CrossRef](#)]
3. Peng, C.Y.; Xing, S.L.; Yuan, Z.Q.; Xiao, J.Y.; Wang, C.Q.; Zeng, J.C. Preparation and anti-icing of superhydrophobic PVDF coating on a wind turbine blade. *Appl. Surf. Sci.* **2012**, *259*, 764–768. [[CrossRef](#)]
4. Wang, Z.W.; Su, Y.L.; Li, Q.; Liu, Y.; She, Z.X.; Chen, F.N.; Li, L.Q.; Zhang, X.X.; Zhang, P. Researching a highly anti-corrosion superhydrophobic film fabricated on AZ91D magnesium alloy and its anti-bacteria adhesion effect. *Mater. Charact.* **2015**, *99*, 200–209. [[CrossRef](#)]
5. Cao, W.T.; Liu, Y.J.; Ma, M.G.; Zhu, J.F. Facile preparation of robust and superhydrophobic materials for self-cleaning and oil/water separation. *Colloids Surf. A* **2017**, *529*, 18–25. [[CrossRef](#)]
6. Liang, W.D.; Wu, Y.; Sun, H.X.; Zhu, Z.Q.; Chen, P.S.; Yang, B.P.; Li, A. Halloysite clay nanotubes based phase change material composites with excellent thermal stability for energy saving and storage. *RSC Adv.* **2016**, *6*, 19669–19675. [[CrossRef](#)]
7. Fan, L.; Li, B.C.; Wang, Q.; Wang, A.Q.; Zhang, J.P. Superhydrophobic gated polyorganosilanes/halloysite nanocontainers for sustained drug release. *Adv. Mater. Interfaces* **2014**, *1*. [[CrossRef](#)]
8. Sun, T.; Feng, L.; Gao, X.; Jiang, L. Bioinspired surfaces with special wettability. *Acc. Chem. Res.* **2006**, *39*, 644–652. [[CrossRef](#)]
9. Cassie, A.B.D.; Baxter, S. Wettability of porous surfaces. *Trans. Faraday Soc.* **1944**, *40*, 546–551. [[CrossRef](#)]
10. Shah, S.M.; Zulfiqar, U.; Hussain, S.Z.; Ahmad, I.; Habib-ur-Rehman; Hussain, I.; Subhani, T. A durable superhydrophobic coating for the protection of wood materials. *Mater. Lett.* **2017**, *203*, 17–20. [[CrossRef](#)]
11. Liu, L.; Lei, J.L.; Li, L.J.; Zhang, R.; Mi, N.Y.; Chen, H.R.; Huang, D.; Li, N.B. A facile method to fabricate the superhydrophobic magnetic sponge for oil-water separation. *Mater. Lett.* **2017**, *195*, 66–70. [[CrossRef](#)]
12. Cao, H.; Gu, W.H.; Fu, J.Y.; Liu, Y.; Chen, S.G. Preparation of superhydrophobic/oleophilic copper mesh for oil-water separation. *Appl. Surf. Sci.* **2017**, *412*, 599–605. [[CrossRef](#)]
13. Wang, L.; Xi, G.H.; Wan, S.J.; Zhao, C.H.; Liu, X.D. Asymmetrically superhydrophobic cotton fabrics fabricated by mist polymerization of lauryl methacrylate. *Cellulose* **2014**, *21*, 2983–2994. [[CrossRef](#)]
14. Lee, J.W.; Park, S.J.; Kim, Y.H. Improvement of interfacial adhesion of incorporated halloysite-nanotubes in fiber-reinforced epoxy-based composites. *Appl. Sci.* **2017**, *7*, 441. [[CrossRef](#)]
15. Massaro, M.; Colletti, C.G.; Lazzara, G.; Milioto, S.; Noto, R.; Riela, S. Halloysite nanotubes as support for metal-based catalysts. *J. Mater. Chem. A* **2017**, *5*, 13276–13293. [[CrossRef](#)]
16. Rizzo, C.; Arrigo, R.; D’Anna, F.; Di Blasi, F.; Dintcheva, N.T.; Lazzara, G.; Parisi, F.; Riela, S.; Spinelli, G.; Massaro, M. Hybrid supramolecular gels of fmoc-f/halloysite nanotubes: Systems for sustained release of camptothecin. *J. Mater. Chem. B* **2017**, *5*, 3217–3229. [[CrossRef](#)]
17. Massaro, M.; Riela, S.; Cavallaro, G.; Colletti, C.G.; Milioto, S.; Noto, R.; Lazzara, G. Eco-compatible halloysite/cucurbit[8]uril hybrid as efficient nanosponge for pollutants removal. *Chemistryselect* **2016**, *1*, 1773–1779. [[CrossRef](#)]
18. Massaro, M.; Lazzara, G.; Milioto, S.; Noto, R.; Riela, S. Covalently modified halloysite clay nanotubes: Synthesis, properties, biological and medical applications. *J. Mater. Chem. B* **2017**, *5*, 2867–2882. [[CrossRef](#)]
19. Yuan, P.; Tan, D.Y.; Annabi-Bergaya, F. Properties and applications of halloysite nanotubes: Recent research advances and future prospects. *Appl. Clay Sci.* **2015**, *112*, 75–93. [[CrossRef](#)]
20. Wu, H.; Watanabe, H.; Ma, W.; Fujimoto, A.; Higuchi, T.; Uesugi, K.; Takeuchi, A.; Suzuki, Y.; Jinnai, H.; Takahara, A. Robust liquid marbles stabilized with surface-modified halloysite nanotubes. *Langmuir* **2013**, *29*, 14971–14975. [[CrossRef](#)] [[PubMed](#)]
21. Zhang, F.; Shi, Z.W.; Chen, L.S.; Jiang, Y.J.; Xu, C.Y.; Wu, Z.H.; Wang, Y.Y.; Peng, C.S. Porous superhydrophobic and superoleophilic surfaces prepared by template assisted chemical vapor deposition. *Surf. Coat. Technol.* **2017**, *315*, 385–390. [[CrossRef](#)]
22. Kavalenka, M.N.; Vulliers, F.; Lischker, S.; Zeiger, C.; Hopf, A.; Rohrig, M.; Rapp, B.E.; Worgull, M.; Holscher, H. Bioinspired air-retaining nanofur for drag reduction. *ACS Appl. Mater. Interfaces* **2015**, *7*, 10651–10655. [[CrossRef](#)] [[PubMed](#)]
23. Ji, H.Y.; Chen, G.; Yang, J.; Hu, J.; Song, H.J.; Zhao, Y.T. A simple approach to fabricate stable superhydrophobic glass surfaces. *Appl. Surf. Sci.* **2013**, *266*, 105–109. [[CrossRef](#)]
24. Menga, N.; Di Mundo, R.; Carbone, G. Soft blasting of fluorinated polymers: The easy way to superhydrophobicity. *Mater. Des.* **2017**, *121*, 414–420. [[CrossRef](#)]

25. Su, D.; Huang, C.Y.; Hu, Y.; Jiang, Q.W.; Zhang, L.; Zhu, Y.F. Preparation of superhydrophobic surface with a novel sol-gel system. *Appl. Surf. Sci.* **2011**, *258*, 928–934. [[CrossRef](#)]
26. Li, C.P.; Li, X.Y.; Duan, X.L.; Li, G.J.; Wang, J.Q. Halloysite nanotube supported Ag nanoparticles heteroarchitectures as catalysts for polymerization of alkylsilanes to superhydrophobic silanol/siloxane composite microspheres. *J. Colloid Interface Sci.* **2014**, *436*, 70–76. [[CrossRef](#)] [[PubMed](#)]
27. Liu, M.X.; Jia, Z.X.; Liu, F.; Jia, D.M.; Guo, B.C. Tailoring the wettability of polypropylene surfaces with halloysite nanotubes. *J. Colloid Interface Sci.* **2010**, *350*, 186–193. [[CrossRef](#)] [[PubMed](#)]
28. Lee, B.P.; Messersmith, P.B.; Israelachvili, J.N.; Waite, J.H. Mussel-inspired adhesives and coatings. *Annu. Rev. Mater. Res.* **2011**, *41*, 99–132. [[CrossRef](#)] [[PubMed](#)]
29. Hong, G.H.; Meng, Y.; Yang, Z.X.; Cheng, H.T.; Zhang, S.B.; Song, W. Mussel-inspired polydopamine modification of bamboo fiber and its effect on the properties of bamboo fiber/polybutylene succinate. *BioResources* **2017**, *12*, 8419–8442. [[CrossRef](#)]
30. Liu, Y.L.; Ai, K.L.; Lu, L.H. Polydopamine and its derivative materials: Synthesis and promising applications in energy, environmental, and biomedical fields. *Chem. Rev.* **2014**, *114*, 5057–5115. [[CrossRef](#)] [[PubMed](#)]
31. Feng, J.R.; Fan, H.L.; Zha, D.A.; Wang, L.; Jin, Z.X. Characterizations of the formation of polydopamine-coated halloysite nanotubes in various pH environments. *Langmuir* **2016**, *32*, 10377–10386. [[CrossRef](#)] [[PubMed](#)]
32. Chao, C.; Liu, J.D.; Wang, J.T.; Zhang, Y.W.; Zhang, B.; Zhang, Y.T.; Xiang, X.; Chen, R.F. Surface modification of halloysite nanotubes with dopamine for enzyme immobilization. *ACS Appl. Mater. Interfaces* **2013**, *5*, 10559–10564. [[CrossRef](#)] [[PubMed](#)]
33. Yah, W.O.; Xu, H.; Soejima, H.; Ma, W.; Lvov, Y.; Takahara, A. Biomimetic dopamine derivative for selective polymer modification of halloysite nanotube lumen. *J. Am. Chem. Soc.* **2012**, *134*, 12134–12137. [[CrossRef](#)] [[PubMed](#)]
34. Di Mundo, R.; Palumbo, F.; D’Agostino, R. Nanotexturing of polystyrene surface in fluorocarbon plasmas: From sticky to slippery superhydrophobicity. *Langmuir* **2008**, *24*, 5044–5051. [[CrossRef](#)] [[PubMed](#)]
35. Wang, Z.X.; Xu, Y.C.; Liu, Y.Y.; Shao, L. A novel mussel-inspired strategy toward superhydrophobic surfaces for self-driven crude oil spill cleanup. *J. Mater. Chem. A* **2015**, *3*, 12171–12178. [[CrossRef](#)]
36. Zhang, L.; Wu, J.J.; Wang, Y.X.; Long, Y.H.; Zhao, N.; Xu, J. Combination of bioinspiration: A general route to superhydrophobic particles. *J. Am. Chem. Soc.* **2012**, *134*, 9879–9881. [[CrossRef](#)] [[PubMed](#)]
37. Zhu, Q.; Pan, Q.M. Mussel-inspired direct immobilization of nanoparticles and application for oil-water separation. *ACS Nano* **2014**, *8*, 1402–1409. [[CrossRef](#)] [[PubMed](#)]
38. Huang, J.Y.; Li, S.H.; Ge, M.Z.; Wang, L.N.; Xing, T.L.; Chen, G.Q.; Liu, X.F.; Al-Deyab, S.S.; Zhang, K.Q.; Chen, T.; et al. Robust superhydrophobic TiO₂@fabrics for UV shielding, self-cleaning and oil-water separation. *J. Mater. Chem. A* **2015**, *3*, 2825–2832. [[CrossRef](#)]
39. Atluri, R.; Hedin, N.; Garcia-Bennett, A.E. Nonsurfactant supramolecular synthesis of ordered mesoporous silica. *J. Am. Chem. Soc.* **2009**, *131*, 3189–3191. [[CrossRef](#)] [[PubMed](#)]
40. Atluri, R.; Iqbal, M.N.; Bacsik, Z.; Hedin, N.; Villaescusa, L.A.; Garcia-Bennett, A.E. Self-assembly mechanism of folate-templated mesoporous silica. *Langmuir* **2013**, *29*, 12003–12012. [[CrossRef](#)] [[PubMed](#)]
41. Gaaz, T.S.; Sulong, A.B.; Kadhum, A.A.H.; Nassir, M.H.; Al-Amiery, A.A. Impact of sulfuric acid treatment of halloysite on physico-chemic property modification. *Materials* **2016**, *9*, 620. [[CrossRef](#)] [[PubMed](#)]
42. Chao, C.; Zhang, B.; Zhai, R.; Xiang, X.; Liu, J.; Chen, R. Natural nanotube-based biomimetic porous microspheres for significantly enhanced biomolecule immobilization. *ACS Sustain. Chem. Eng.* **2014**, *2*, 396–403. [[CrossRef](#)]
43. Hebbar, R.S.; Isloor, A.M.; Ananda, K.; Ismail, A.F. Fabrication of polydopamine functionalized halloysite nanotube/polyetherimide membranes for heavy metal removal. *J. Mater. Chem. A* **2016**, *4*, 764–774. [[CrossRef](#)]
44. Zhu, X.; Li, H.; Liu, H.; Peng, W.; Zhong, S.; Wang, Y. Halloysite-based dopamine-imprinted polymer for selective protein capture. *J. Sep. Sci.* **2016**, *39*, 2431–2437. [[CrossRef](#)] [[PubMed](#)]
45. Gaaz, T.S.; Sulong, A.B.; Kadhum, A.A.H.; Nassir, M.H.; Al-Amiery, A.A. Surface improvement of halloysite nanotubes. *Appl. Sci.* **2017**, *7*, 291. [[CrossRef](#)]
46. Yuan, P.; Southon, P.D.; Liu, Z.; Green, M.E.R.; Hook, J.M.; Antill, S.J.; Kepert, C.J. Functionalization of halloysite clay nanotubes by grafting with gamma-aminopropyltriethoxysilane. *J. Phys. Chem. C* **2008**, *112*, 15742–15751. [[CrossRef](#)]

47. Kang, H.J.; Liu, X.R.; Zhang, S.F.; Li, J.Z. Functionalization of halloysite nanotubes (HNTs) via mussel-inspired surface modification and silane grafting for HNTs/soy protein isolate nanocomposite film preparation. *RSC Adv.* **2017**, *7*, 24140–24148. [[CrossRef](#)]
48. Raman, V.S.; Rooj, S.; Das, A.; Stöckelhuber, K.W.; Simon, F.; Nando, G.B.; Heinrich, G. Reinforcement of solution styrene butadiene rubber by silane functionalized halloysite nanotubes. *J. Macromol. Sci. Part A Pure Appl. Chem.* **2013**, *50*, 1091–1106. [[CrossRef](#)]
49. Zangmeister, R.A.; Morris, T.A.; Tarlov, M.J. Characterization of polydopamine thin films deposited at short times by autoxidation of dopamine. *Langmuir* **2013**, *29*, 8619–8628. [[CrossRef](#)] [[PubMed](#)]
50. Han, Y.; Wu, X.; Zhang, X.; Zhou, Z.; Lu, C. Dual functional biocomposites based on polydopamine modified cellulose nanocrystal for Fe³⁺-pollutant detecting and autoblocking. *ACS Sustain. Chem. Eng.* **2016**, *4*, 5667–5673. [[CrossRef](#)]
51. Wang, P.; Du, M.L.; Zhang, M.; Zhu, H.; Bao, S.Y.; Zou, M.L.; Yang, T.T. Facile fabrication of AuNPs/PANI/HNTs nanostructures for high-performance electrochemical sensors towards hydrogen peroxide. *Chem. Eng. J.* **2014**, *248*, 307–314. [[CrossRef](#)]
52. Liu, C.Y.; Wang, S.L.; Shi, J.Y.; Wang, C.Y. Fabrication of superhydrophobic wood surfaces via a solution-immersion process. *Appl. Surf. Sci.* **2011**, *258*, 761–765. [[CrossRef](#)]
53. Yu, H.; Gao, J.; Chen, Y.; Zhao, Y. Preparation and properties of stearic acid/expanded graphite composite phase change material for low-temperature solar thermal application. *J. Therm. Anal. Calorim.* **2016**, *124*, 87–92. [[CrossRef](#)]
54. Giro-Paloma, J.; Martinez, M.; Cabeza, L.F.; Ines Fernandez, A. Types, methods, techniques, and applications for microencapsulated phase change materials (MPCM): A review. *Renew. Sustain. Energy Rev.* **2016**, *53*, 1059–1075. [[CrossRef](#)]
55. Kenisarin, M.M.; Kenisarina, K.M. Form-stable phase change materials for thermal energy storage. *Renew. Sustain. Energy Rev.* **2012**, *16*, 1999–2040. [[CrossRef](#)]
56. Mei, D.; Zhang, B.; Liu, R.; Zhang, H.; Liu, J. Preparation of stearic acid/halloysite nanotube composite as form-stable PCM for thermal energy storage. *Int. J. Energy Res.* **2011**, *35*, 828–834. [[CrossRef](#)]
57. Zhao, Y.F.; Abdullayev, E.; Vasiliev, A.; Lvov, Y. Halloysite nanotubule clay for efficient water purification. *J. Colloid Interface Sci.* **2013**, *406*, 121–129. [[CrossRef](#)] [[PubMed](#)]



© 2017 by the authors. Licensee MDPI, Basel, Switzerland. This article is an open access article distributed under the terms and conditions of the Creative Commons Attribution (CC BY) license (<http://creativecommons.org/licenses/by/4.0/>).